

DESIGN CONSIDERATIONS FOR THE EXTRACTION LINE OF THE PROPOSED THIRD BEAMLINE PORTHOS AT SwissFEL

S. Reiche*, P. Craievich, M. Schär, T. Schietinger
Paul Scherrer Institut, Villigen PSI, Switzerland

Abstract

It is planned to extend SwissFEL by a third beamline, named Porthos, operating in the hard X-ray regime. Three bunches will be accelerated within one RF pulse and distributed into the different beamlines with resonant kickers operating at the bunch spacing of a few tens of nanoseconds. While the full extent of Porthos will not be realized before the end of this decade, the extraction line from the main linac will also serve the P^3 (PSI Positron Production) experiment for the demonstration of a possible positron source for the FCC-ee project at CERN. We present the design of the switchyard, which will serve both purposes with only minimal changes.

INTRODUCTION

The free-electron laser (FEL) facility SwissFEL [1] at the Paul Scherrer Institute drives the two independent undulator beamlines Athos and Aramis for the soft and hard X-ray range, respectively. Two electron bunches are generated in the SwissFEL RF photogun within the same RF pulse, accelerated up to the GeV range and compressed in two stages. At 3.2 GeV the second bunch is extracted from the main linac and transported to the Athos undulator, while the other bunch is accelerated further to reach beam energies of up to 6 GeV. Since SwissFEL has demonstrated that multiple beamlines can be operated at the same repetition rate as the RF system, it is planned to extend the facility by a third beamline, called Porthos. Its extraction shares many similarities with the Athos extraction but is placed at the end of the existing linac, putting the operation range of Porthos into the hard X-ray regime. A schematic layout of SwissFEL with the planned third beamline is shown in Fig. 1.

In this contribution we describe the design strategies for the extraction line and its synergy with a planned experiment, named P^3 for “PSI Positron Production” [2], to demonstrate the positron yield for a possible positron source for the FCC project [3].

EXPERIENCE FROM THE ATHOS EXTRACTION LINE

Since the extraction lines for Porthos and Athos share the same purpose they follow the same design guideline. Since we already gained some experience with the operation of the Athos line, we may apply this knowledge to improve upon the design and to eliminate potential bottlenecks in performance and operation.

Design Principle

In SwissFEL two electron bunches are generated and accelerated within a single RF pulse. At an energy of about 3.2 GeV and after two stages of bunch compression a resonant kicker system operating at 17.8 MHz [4] extracts the second bunch from the main linac and sends it into the Athos extraction line. Since the time separation between the two bunches is only 28 ns the combination of a kick in the vertical direction for an offset of 10 mm and a Lambertson septum [5], which steers the beam horizontally, offers optimal performance. The other bunch travels on a straight path, passing through a hole in the lower yoke of the septum magnet.

The extraction line provides an offset of 3.75 m for the Athos beamline with respect to the main linac and Aramis beamline. The transport consists of two sections with a total bending angle of 5° and -5°, respectively, and a straight middle section with its length matched to the overall offset. The dispersion function should be closed in the middle section for reducing constraints on the Swiss function between the two bending sections.

The design [6] solves three problems to preserve the beam quality needed to drive the soft X-ray beamline Athos. The first problem is the closure of the vertical dispersion, originating at the resonant kicker. Since it is impractical to generate an offset without dispersion in a short distance before the Lambertson septum, the vertical dispersion leaks through the first bending section and is then caught by a downward dogleg. Two quadrupoles within the dogleg close the vertical dispersion function after the second dogleg dipole. The tunability is limited and requires values for the dispersion functions η_y and η'_y close to those at the Lambertson septum entrance.

The second problem is the residual R_{56} for the simplest solution of a double-bend system—two bending dipoles and a center quadrupole with a focal length half the distance between the bending magnets. It decompresses any bunch with a residual energy chirp from the last compression stage. Without compensating this intrinsic R_{56} of the double-bend system, the electron bunch needs to be compressed stronger to compensate for the elongation by the extraction line. The coherent synchrotron radiation (CSR) [7] effects are unnecessarily stronger and the risk of electron beam quality degradation is high. The Athos extraction design compensates it by a weak center dipole and a total bending of 2° by the Lambertson magnet, 1° by the center dipole and again 2° by the last bending magnet of the first section. The beam transport ensures that the sign of the dispersion function η_x changes for the center dipole and is inverted back for a

* sven.reiche@psi.ch

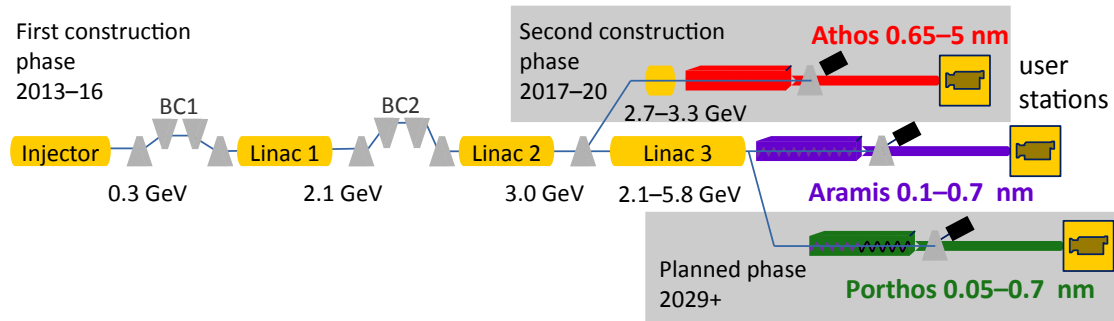


Figure 1: Schematic layout of the SwissFEL Facility.

complete closure after the last dipole. Thus the focusing strength of the quadrupole defines the net R_{56} value while the dipoles are operated at fixed deflection angles.

The third problem is the compensation and mitigation of the transverse kicks of the CSR in each horizontal bending dipole. The angle for the vertical dogleg is small and the effect on the beam negligible. The general guideline calls for minimizing the betatron function β_x in each bending magnet to a value of around 1 to 2 m. In addition, the betatron phase advance between the two bending sections is tuned so that the opposite signs of the kicks cancel each other.

Experience

The main drawback in the Athos extraction line is the limited flexibility in the beam transport due to the center dipole. In a simple bend-quadrupole-bend system only a betatron phase advance of 180° is needed if the betatron-function values β_x are small at the entrance and exit of the bending section due to the mitigation of the transverse CSR kicks. It resembles a simple point-to-point imaging system. An additional benefit is that with the CSR acting in the same direction the 180° phase advance already compensates the kick in first order. In a triple-bend system, such as in Athos, the flip in the dispersion function for the center dipole requires much more than 360° betatron phase advance. Thus the intrinsic kick compensation is lost. However, the beam transport in the vertical plane is even more problematic, since it should provide a similar phase advance in the vertical plane. It is difficult to place defocusing quadrupoles in the bending section without reducing the phase advance in the horizontal plane. The outcome are very large betatron function values at the quadrupole location while operating in a nearly unstable beam transport lattice. Small errors in the quadrupole strengths have a large impact on the betatron function along the extraction line and the matching at the undulator entrance can be lost easily.

These days we follow a different configuration where we do not flip the sign of the dispersion function η_x anymore. The enhanced decompression by the center dipole is compensated by leaking out dispersion from the first bending section through the straight section and closing it only after the second bending section. This gives us a larger flexibility

on tuning the net R_{56} while keeping the maximum values of the betatron function below 80 m.

PORTHOS EXTRACTION LINE DESIGN

Figure 2 shows the principal components, such as quadrupoles and dipoles, for the proposed extraction line of Porthos. The design addresses the major restriction of the Athos design, which is the control of the overall R_{56} without large optics function values and an unstable beam transport. There are two possible solutions: First, a reverse bend for the center dipole. This eliminates the need to flip the sign of the dispersion function η_x . However the overall deflecting strengths of the outer dipoles are larger. Instead of the Athos configuration with deflections of (2°, 1°, 2°), a possible solution with a reverse bend would be (2.7°, -0.4°, 2.7°), but there remains a strong coupling between optics and net compression. The second solution, which is the one favored for Porthos, is to use a fixed double-bend system with net decompression and to compensate with a normal four-dipole chicane. Since the natural focusing of the chicane is very small, we have a ‘knob’ to control the R_{56} independently from the optics function.

With the R_{56} control removed from the bending sections, the required number of quadrupoles is four per section. The optical functions—both betatron and dispersion—have a mirror symmetry at the center point of the section. The first two quadrupoles enforce the matching condition $\eta'_x = \eta'_y = 0$, while the matching quadrupoles upstream of the Lambertson septum do the same for the optical function ($\alpha_x = \alpha_y = 0$). The positions have been roughly optimized to provide balanced focusing for both planes. The betatron function β_x has a value of about 1 m at the location of the septum and the last dipole. The last bending section has the same layout and uses the same quadrupole strengths as the first, although the already closed vertical dispersion would allow for a more compact solution in principle. In between the two bending sections there is the downward dogleg closing the vertical dispersion and compensating the 10 mm offset from the resonant kick upstream of the extraction line. Figure 3 shows the betatron and dispersion functions along the extraction line. The Lambertson septum is placed at the orbit coordinate $s = 429$ m.

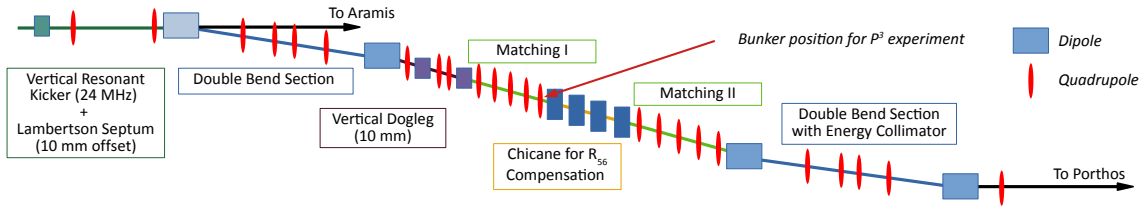


Figure 2: Components in the Porthos extraction line.

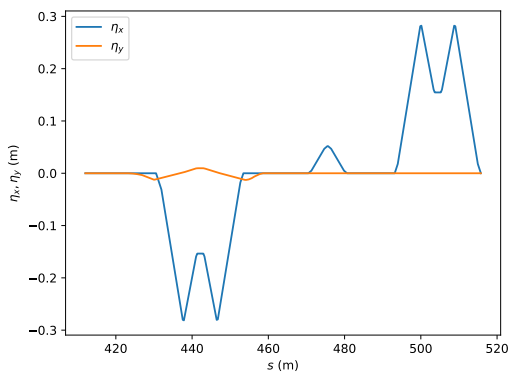
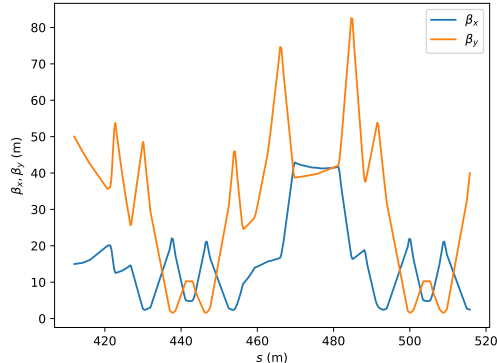
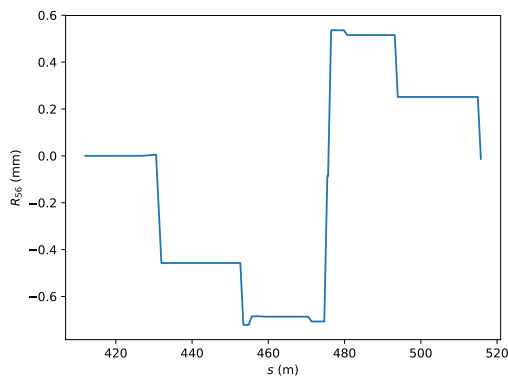
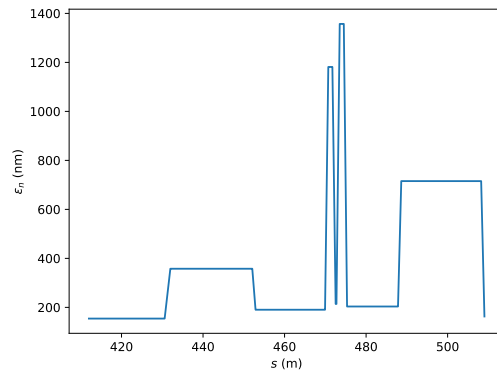


Figure 3: Betatron and dispersion functions along the Porthos extraction line (upper and lower plot, respectively).

Figure 4: R_{56} value for isochronous operation.

The main dipoles have a deflection angle of 2.55° , which is driven by the available space in the SwissFEL tunnel while providing the longest possible space between the exit of the extraction line and the position of the Porthos beam dump. The downward dogleg features an angle of 0.2° while the chicane in the middle has an angle of 0.71° for isochronous operation (Fig. 4). The location also favors the mitigation of the microbunching instability [8]. Any accumulated energy modulation by the induced microbunching from the first bending section is reversed since the chicane enforces a bunching at the opposite phase. Thus the second half of the extraction line removes the energy modulation from the first half. The R_{56} can be fine-tuned to minimize the microbunching content in general.

Figure 5: Normalized emittance in x along the extraction line.

We performed Elegant simulations [9] to estimate the impact of CSR by tracking a 200 pC bunch with a Gaussian current distribution and an rms duration of 40 fs, cut at ± 40 fs. In general, small beta functions in the main dipole help to mitigate the emittance increase by the kicks but an effect is still noticeable. For the chicane a large betatron function value is chosen with little phase advance so that the net CSR kick is small. The effect on the normalized emittance is shown in Fig. 5. The growth is about 5% for an initial projected emittance of 180 nm. The efficiency in this compensation is shown in Fig. 6 where the phase space distributions in the t - x and t - x' planes are shown in the last bending section (left plots) and the exit (right plots). At the energy collimator position (left plots) there is a strong variation in x visible along the bunch, much larger than the

intrinsic beam size. It increases the projected emittance up to 700 nm (see Fig. 5 at $s = 500$ m). With the last CSR kick added in the last dipole of the switchyard (right plots) this variation along the bunch is removed and the initial projected emittance is mostly recovered. The emittance growth for a 20 fs bunch is about 20% but can be further optimized with the phase advance in the bending section and in between them.

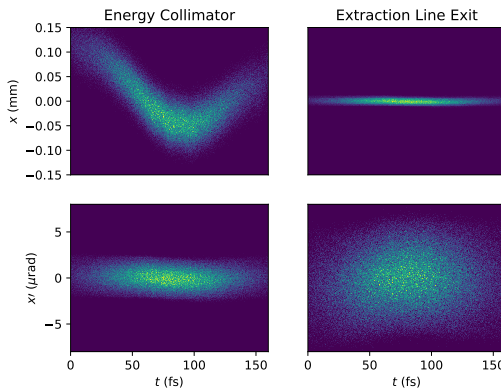


Figure 6: Time-resolved electron beam distributions in x and x' in the center of the last bending section (energy collimator) and at the exit of the transport line (left and right plot, respectively).

The energy loss by CSR cannot be compensated and adds up for each dipole. For the truncated Gaussian distribution of 40 fs rms length the variation in energy loss is about 4 MeV. The effective loss potential depends on the current profile [10] and flatter profiles, such as at SwissFEL with the leading and trailing horn cut away in the first bunch compressor, the variation is significantly reduced.

The final layout has sufficient space, about 20 m, for placing accelerating cavities. This would increase the operating beam energy of Porthos enabling higher photon energies, without sacrificing space in the beamline between extraction end and beam dump.

POSITRON PRODUCTION EXPERIMENT P^3 AT SwissFEL

Since the Porthos beamline will not be implemented until the period 2029 to 2032, an early realization of the extraction line is required to drive the P^3 experiment. The positron source will be set up in a bunker with a footprint of roughly 10×4 m near the center of the new beam line. The energy of 6 GeV of the SwissFEL electron beam corresponds to the drive beam energy in the baseline design of the FCC-ee injector complex and makes it the natural candidate to drive a positron source demonstrator. Recent advances in high-temperature superconductors (HTS) allow for a highly efficient matching of the extremely large positron emittance at the exit of the production target through an on-axis solenoidal field of more than 10 T. In addition to this device, the P^3 experiment envisages the use of two S-band

standing-wave RF cavities with a large radial aperture of 20 mm surrounded by a multi-Tesla field generated by conventional superconducting solenoids. Simulations show that these key devices can increase the positron capture efficiency at the end of the experiment by up to 75%. This corresponds to an estimated positron yield of 8 positrons per electron at the damping ring of the FCC-ee injector complex, an improvement of about an order of magnitude compared to the state-of-the-art at SuperKEKB.

Based on the final layout of the extraction line the realization for the P^3 experiment should be consistent without any major changes in the type and position of its components. Since the experiment has dedicated beam development shifts, there is no need for a resonant kicker and the Lambertson extraction. Thus the Lambertson is replaced temporarily with a spare dipole, which deflects the beam by 2.55° . Also, the beam elevation by 10 mm due to the resonant kicker up to the downward dogleg is excluded in the initial realization. Since the experiment will operate with an uncompressed bunch with a few ps rms pulse duration, there is no need for corrector magnets for CSR kick compensation either. Five quadrupoles after the bending section will control the beam size at the target location of the experiment in a range between 20 and 1000 μ m. Therefore the initial implementation of the extraction line consists of two dipole magnets, about nine quadrupole magnets, steerer magnets and some basic instrumentation like beam position monitors and screens, up to the point where the beam enters the experimental chamber.

CONCLUSION

The proposed P^3 experiment to demonstrate the positron yield for a future FCC position source benefits from an early realization of the extraction line for the third FEL beamline Porthos at SwissFEL, scheduled for construction between 2029 and 2032. Therefore, initial design studies for the Porthos layout have been done to extract an electron bunch while preserving its brightness. The design benefits also from the experience at the existing extraction line for the soft X-ray beamline Athos, avoiding any strong coupling between dispersion and optics function. The implementation of the extraction line will start in 2023 with only selected components, sufficient to transport a 6 GeV electron beam to the experimental target of the P^3 experiment.

REFERENCES

- [1] E. Prat *et al.*, “A compact and cost-effective hard X-ray free-electron laser driven by a high-brightness and low-energy electron beam,” *Nat. Photonics*, vol. 14, no. 12, pp. 748–754, 2020. doi: 10.1038/s41566-020-00712-8
- [2] P. Craievich, M. Schaer, N. Vallis, and R. Zennaro, “FCC-ee Injector Study and the P3 Project at PSI,” *CHART Scientific Report 2021*, pp. 1–47, 2021. <https://chart.ch/wp-content/uploads/2022/05/Chart-Scientific-Report-2021-FCCee-Injector.pdf>
- [3] I. Chaikovska *et al.*, “Positron Source for FCC-ee,” in *Proc. IPAC’19*, Melbourne, Australia, May 2019, pp. 424–427. doi: 10.18429/JACoW-IPAC2019-MOPMP003

[4] M. Paraliev and C. H. Gough, "Resonant Kicker System With Sub-part-per-million Amplitude Stability," in *Proc. IPAC'17*, Copenhagen, Denmark, May 2017, pp. 3174–3177.
doi:10.18429/JACoW-IPAC2017-WEPIK098

[5] G. R. Lambertson, "Charged particle extracting magnet for an accelerator," US3323088A, 1967. <https://patents.google.com/patent/US3323088/en>

[6] N. Milas and S. Reiche, "Switchyard Design: Athos," in *Proc. FEL'12*, Nara, Japan, Aug. 2012, pp. 109–112. <https://jacow.org/FEL2012/papers/MOPD37.pdf>

[7] E. L. Saldin, E. A. Schneidmiller, and M. V. Yurkov, "On the coherent radiation of an electron bunch moving in an arc of a circle," *Nucl. Instrum. Methods Phys. Res., Sect. A*, vol. 398, no. 2, pp. 373–394, 1997.
doi:10.1016/S0168-9002(97)00822-X

[8] J. Qiang *et al.*, "Design Optimization of Compensation Chicanes in the LCLS-II Transport Lines," in *Proc. IPAC'16*, Busan, Korea, May 2016, pp. 1695–1698.
doi:10.18429/JACoW-IPAC2016-TUPOR018

[9] M. Borland, "ELEGANT: A flexible SDDS-compliant code for accelerator simulation," Argonne National Lab., IL (US), Tech. Rep. LS-287, 2000. doi:10.2172/761286

[10] C. Mitchell, J. Qiang, and P. Emma, "Longitudinal pulse shaping for the suppression of coherent synchrotron radiation-induced emittance growth," *Phys. Rev. ST Accel. Beams*, vol. 16, no. 6, p. 060 703, 2013.
doi:10.1103/PhysRevSTAB.16.060703